Acta Crystallographica Section D
Biological Crystallography
ISSN 1399-0047

Temperature-dependent radiation sensitivity and order of 70S ribosome crystals

Matthew Warkentin,[a]* Jesse B. Hopkins,[a] Jonah B. Haber,[a] Gregor Blaha[b] and Robert E. Thorne[a]

[a]Physics Department, Cornell University, Ithaca, NY 14853, USA, and [b]Department of Biochemistry, University of California, Riverside, CA 92521, USA

Correspondence e-mail: maw64@cornell.edu

Received 4 December 2013
Accepted 1 August 2014

All evidence to date indicates that at T = 100 K all protein crystals exhibit comparable sensitivity to X-ray damage when quantified using global metrics such as change in scaling B factor or integrated intensity *versus* dose. This is consistent with observations in cryo-electron microscopy, and results because nearly all diffusive motions of protein and solvent, including motions induced by radiation damage, are frozen out. But how do the sensitivities of different proteins compare at room temperature, where radiation-induced radicals are free to diffuse and protein and lattice structures are free to relax in response to local damage? It might be expected that a large complex with extensive conformational degrees of freedom would be more radiation sensitive than a small, compact globular protein. As a test case, the radiation sensitivity of 70S ribosome crystals has been examined. At T = 100 and 300 K, the half doses are 64 MGy (at 3 Å resolution) and 150 kGy (at 5 Å resolution), respectively. The maximum tolerable dose in a crystallography experiment depends upon the initial or desired resolution. When differences in initial data-set resolution are accounted for, the former half dose is roughly consistent with that for model proteins, and the 100/300 K half-dose ratio is roughly a factor of ten larger. 70S ribosome crystals exhibit substantially increased resolution at 100 K relative to 300 K owing to cooling-induced ordering and not to reduced radiation sensitivity and slower radiation damage.

1. Introduction

Most studies of global radiation damage to macromolecular crystals have focused on well behaved and well packed model proteins such as lysozyme, thaumatin, ferritin and insulin. Initial studies focused on T = 100 K (Teng & Moffat, 2000, 2002; Kmetko *et al.*, 2006; Owen *et al.*, 2006) and room-temperature measurements (Blake & Phillips, 1962; Southworth-Davies *et al.*, 2007; Barker *et al.*, 2009; Kmetko *et al.*, 2011; Owen *et al.*, 2012). Improved sample preparation and cooling methods have recently allowed the full temperature dependence to be characterized (Warkentin & Thorne, 2010). At 100 K, all protein crystals have been found to exhibit comparable global radiation sensitivities on a per-dose basis, consistent with results from cryoelectron microscopy (Henderson, 1990), with typical dose limits of 15–30 MGy (Teng & Moffat, 2000, 2002; Owen *et al.*, 2006; Kmetko *et al.*, 2006). Anecdotal evidence also suggests that crystals are orders of magnitude more radiation sensitive at room temperature and that some crystals are considerably more radiation sensitive than others. However, measurements of model proteins show that they are 'only' 30–50 times more sensitive (as quantified by dose-dependent increases in scaling B factors) at room temperature and that protein-to-protein

variations, while larger than at T = 100 K, are still modest (Southworth-Davies *et al.*, 2007; Barker *et al.*, 2009; Warkentin & Thorne, 2010; Kmetko *et al.*, 2011; Owen *et al.*, 2012).

A nagging concern has been how well do these results for well behaved, compact and well packed model proteins generalize to more flexible, more dynamic and/or less well packed structures of significant biological interest? To answer these questions, we have examined the global radiation sensitivity of 70S ribosome crystals at 100, 180 and 300 K and have explored the time evolution of damage at room temperature.

Although nearly all crystallography is currently performed at T = 100 K, a large expansion in near-room-temperature data collection is certain to occur in the coming decade owing to technical advances in hardware and crystallographic data-processing software that have made room-temperature data collection and analysis much easier, owing to ultrahigh-throughput sample-handling methods for room-temperature diffraction screening currently under development and owing to a drive to obtain more accurate and detailed information about room/biological temperature conformations and ensembles relevant to, for example, understanding the mechanisms of allostery (Fraser *et al.*, 2009, 2011). Quantifying and understanding both the low-temperature and especially the room-temperature variability in radiation sensitivity among proteins, and especially the behavior of large, dynamic complexes whose room-temperature X-ray crystallographic study is likely to be most illuminating, is essential to these efforts.

2. Methods

70S ribosome from *Thermus thermophilus* was crystallized by vapor diffusion in hanging drops consisting of 2.9%(*w*/*v*) PEG 20 000, 100 m*M* Tris–HCl pH 7.6, 10 m*M* magnesium acetate, 10 m*M* ammonium chloride, 50 m*M* potassium chloride. The crystals were further stabilized by the addition of MPD to a concentration of 40%(*w*/*v*). The stabilized crystals belonged to space group $P2_12_12_1$, with unit-cell parameters a = 210, b = 449, c = 623 Å at T = 100 K as previously described (Selmer *et al.*, 2006).

Typical crystals were 500–1000 µm in length with a ∼200 µm square cross-section. Crystals were mounted on MicroLoops E (MiTeGen, Ithaca, New York, USA), which are loops that were specifically designed for needle-shaped crystals, and oriented to place the long direction perpendicular to the beam. For data collection at T = 100 and 180 K, the mounted crystals were

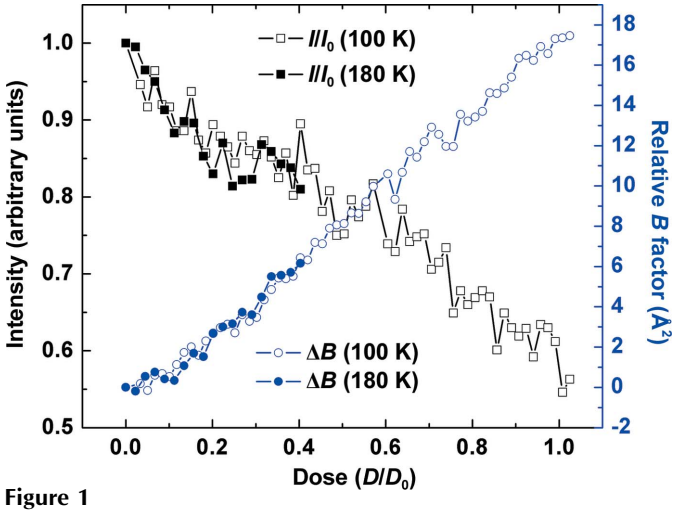

Figure 1
Integrated intensity (black, from *XDS*) and relative *B* factor (blue, from *XSCALE*) *versus* dose at T = 100 and 180 K (samples 1 and 2, respectively) for 70S ribosome crystals. The dose axis has been scaled to D_0 = 50 MGy at 100 K and D_0 = 6.25 MGy at 180 K to facilitate comparison of the dose dependence at these temperatures.

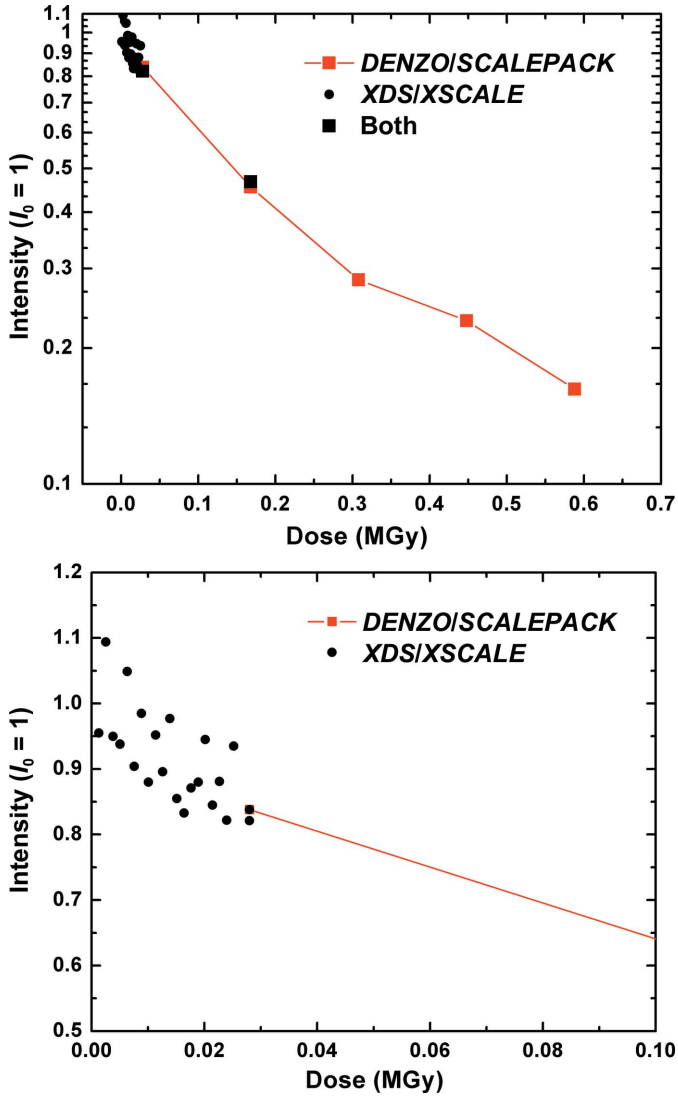

Figure 2
Integrated intensity *versus* dose for a 70S ribosome crystal at 300 K. A series of 20 80 ms exposures were first collected to probe for an ultrafast initial damage/intensity decay rate (solid circles, shown on an expanded dose scale at the bottom). A series of five 10 s exposures was then taken (solid squares) until the crystal was highly disordered (top). The frames could not all be integrated by a single software package. *XDS*/*XSCALE* was successful with the weakly exposed 80 ms frames, while only *DENZO*/*SCALEPACK* worked for the more fully exposed frames. Frames where both packages worked were used to put the two curves on the same scale. The initial diffraction resolution of the crystal was ∼5 Å.

stripped of excess mother liquor and placed directly into the nitrogen-gas cryostream (Oxford Cryosystems, Oxford, England) set to the desired temperature at the beamline. No additional cryoprotectants were added because of the already high MPD concentration of 40%(*w*/*v*). For data collection at room temperature, crystals were placed in a Micro-RT capillary (MiTeGen, Ithaca, New York, USA) containing reservoir solution at one end for vapour stabilization. X-ray diffraction experiments with 12.6 keV/0.98 Å X-rays were performed at the National Synchrotron Light Source using station X25. The beam size was defined by a 100 µm circular collimator and the flux measured using a calibrated ion chamber was 4.2×10^{11} photons s^{-1}. The dose was calculated using *RADDOSE* (Paithankar & Garman, 2010), assuming a top-hat profile, and the dose rate was 15.0 kGy s^{-1}. Diffraction frames were collected with a PILATUS 6M detector (Dectris, Baden, Switzerland). Initial diffraction evaluation was performed on approximately 25 as-grown and MPD-stabilized crystals at 300 K (in part to identify crystals that diffracted with the best possible resolution) and one MPD-stabilized crystal, each at 180 and 100 K. Detailed dose-dependent measurements were then performed on one crystal at each temperature.

At T = 100 and 180 K (Fig. 1), repeated sets of six frames, each with a 10 s exposure and a φ rotation of 0.3° per frame, were taken over the same 1.8° angular wedge. At room temperature, initial measurements using 10 s frames yielded poor diffraction resolution. In the room-temperature data presented here (Fig. 2) the exposure time per frame was 0.08 s for the first 20 frames and was then increased to 10 s for the following five frames, with a dead time between frames of 3.2 ms. The exposure recorded in each frame was spread over a 0.2° wedge, which was the same for each frame. In measurements at all temperatures, the crystals were not translated during data collection. Illuminating only a small angular wedge without sample translation ensures that the illuminated sample volume is uniformly irradiated and maximizes the accuracy and reproducibility of radiation-damage measurements (Schulze-Briese *et al.*, 2005; Kmetko *et al.*, 2006; Meents *et al.*, 2007). Radiation sensitivity was quantified using the half dose (the dose at which the total integrated intensity falls to half of its initial value) and, when the crystal resolution allowed, the *B*-factor sensitivity (the rate of increase of the scaling *B* factor per unit dose).

Diffraction data were processed with *XDS*/*XSCALE* (Kabsch, 2010) and/or *DENZO*/*SCALEPACK* (Otwinowski & Minor, 1997) to obtain the total integrated intensity and, if the data resolution range permitted it, the relative scaling *B* factor. At T = 100 and 180 K, each 1.8° wedge of data was processed independently to determine the total intensities and the wedges were then scaled together to determine the relative scaling *B* factors. The data at room temperature did not extend to a high enough resolution for the *B* factors to be determined.

3. Results

At room temperature, the diffraction resolution was approximately 5–10 Å for the MPD-stabilized crystals and was worse for the as-grown crystals. All of the data reported here are thus for MPD-stabilized crystals. After cooling to 180 or 100 K, the stabilized crystals diffracted to approximately 3 Å resolution. As we will address below, this indicated either that the crystals were so radiation sensitive that a single exposure was enough to severely damage them or that the cryocooling process dramatically improved the crystalline order.

Fig. 1 shows the total integrated intensity and relative *B* factor as a function of dose for two different crystals: one at T = 100 K (sample 1) and one at T = 180 K (sample 2). At T = 100 and 180 K the half doses are 64 and 8.0 MGy and the *B*-factor sensitivities are 0.33 and 2.64 $Å^2\,MGy^{-1}$, respectively. The intensity and *B*-factor data at 180 K have been scaled by a factor of eight (the half-dose ratio) along the dose axis to illustrate that they have the same functional dependence as the data at 100 K.

Fig. 2 shows the total integrated diffraction intensity in Bragg reflections *versus* dose at room temperature for a third crystal (sample 3). The intensities of the initial series of 80 ms exposures collected at the maximum frame rate of the PILATUS 6M detector (12.5 Hz) are indicated by solid circles and the intensities of the final series of five 10 s exposures are indicated by solid squares. The intensities of the two sequences are normalized so that the last point of the initial 80 ms series coincides with the first point of the final 10 s series. The total loss of diffraction intensity during the initial exposure series, lasting 1.6 s, was approximately 15%. The initial slope of intensity *versus* dose measured during this short-exposure series is comparable to that measured during the long-exposure series. The half dose for the observed portion of the decay was 0.15 MGy as determined by direct interpolation of the intensity data in Fig. 2.

4. Discussion

4.1. Origin of the diffraction-resolution improvement on cryocooling

The diffraction resolution of the two cryocooled crystals in Fig. 1 was dramatically better than that of all ∼25 as-grown and MPD-stabilized crystals examined at room temperature (3 *versus* 5–10 Å, as measured using properly exposed 1–10 s acquisition time frames in all cases, not the underexposed 80 ms frames). One possible explanation for the enhanced low-temperature diffraction resolution is that at room temperature the crystals are so radiation sensitive that they are substantially damaged in a single 1–10 s exposure. This 'damage in one shot' hypothesis requires that the resolution is lost in a small fraction of the exposure time and dose per frame; otherwise, the first exposure would contain some faint high-resolution diffraction spots (as is the case in the 'diffract and destroy' approach to crystallography at free-electron laser sources such as the Linac Coherent Light Source; Chapman *et al.*, 2011).

The data in Fig. 2 limit this ultrafast decay time to at most a small fraction of the 80 ms exposure time per frame in the initial 20 frames, and the corresponding dose to a small

fraction of 1.2 kGy. Assuming a crystal density of 1.2 g cm^{-3}, a dose of 1.2 kGy corresponds to the absorption of ~180 12.6 keV photons per μm^3 or of one photon in a volume containing 760 complete 70S units. Assuming a molecular mass of 2.5 MDa and an average of ~6 Da per atom, the energy density deposited in the crystal corresponds to 1 eV in a volume containing ~25 000 ribosome atoms. Based upon prior measurements of the dose dependence of global and site-specific damage to protein crystals and also of damage to proteins in dilute solution (Dertinger & Jung, 1970), it is extremely unlikely that such a small dose could create such a large amount of global damage in such a short time.

An alternative, more likely explanation is that ribosome crystals undergo a structural transformation during cooling that dramatically enhances the crystalline order. This transformation could be *via* an abrupt first-order-like transition at a well defined temperature or possibly *via* a more or less continuous lattice evolution with temperature. Diffraction improvement *via* a cooling-induced structural transformation has been observed in nucleosome crystals plunge-cooled in liquid propane. These crystals can undergo a ~5% unit-cell transformation with an associated improvement in diffraction resolution from 3.4 to 2.9 Å, with a higher propane temperature (153 K) and therefore a slower cooling rate favouring the transformation (Edayathumangalam & Luger, 2005). In the present measurements, the use of nitrogen gas-stream cooling and the relatively large size of the crystals likely gave relatively low (~100 K s^{-1}) cooling rates and relatively long (~1 s) cooling times, perhaps allowing sufficient time for temperature-dependent structural relaxations to proceed before the internal solvent vitrified.

First-order-like structural transformations involving abrupt changes in unit-cell dimensions and diffraction resolution can occur as a function of hydration level near room temperature (Esnouf *et al.*, 1998; Kiefersauer *et al.*, 2000; Dobrianov *et al.*, 2001), providing motivation for the use of variable-humidity gas streams at synchrotron beamlines. Inducing structural transformations using controlled cooling may thus provide another generally useful strategy for improving the order of poorly diffracting crystals.

4.2. Radiation sensitivity at T = 100 K

At T = 100 K, at which data are typically collected in macromolecular crystallography, the ribosome crystal had a half dose of 64 MGy. This compares with T = 100 K half doses of 17 MGy for tetragonal lysozyme (Teng & Moffat, 2002), 21.5 MGy for myrosinase (Burmeister, 2000) and 43 MGy for ferritin (Owen *et al.*, 2006). The *B*-factor sensitivity at 100 K was 0.33 Å^2 MGy^{-1}, which is somewhat smaller than the previously reported values for lysozyme, catalase, thaumatin and apoferritin of 0.94, 0.94, 1.27–1.42 and 1.34 Å^2 MGy^{-1}, respectively (Kmetko *et al.*, 2006; Warkentin & Thorne, 2010), but comparable to an earlier value of 0.4 Å^2 MGy^{-1} reported for lysozyme (Teng & Moffat, 2002). All of these half doses and *B*-factor sensitivities are likely to be accurate to at best a factor of two because of differences in experimental details (including beam size and profile and crystal size and shape), in the accuracy of dose-rate calibrations, and because (for reasons yet to be determined) both half doses and *B*-factor sensitivities vary by roughly a factor of two between crystals of the same protein (Warkentin & Thorne, 2010; Warkentin, Badeau, Hopkins, Mulichak *et al.*, 2012).

4.3. Resolution dependence of radiation sensitivities

The somewhat larger T = 100 K half dose of ribosome crystals can be explained by their relatively poor diffraction resolution limit. In imaging and diffraction, much more damage and a much larger dose is required to disrupt features on, say, the 10 Å scale than on the 1 Å scale; a protein in a crystal will retain its overall shape long after substantial atomic-scale damage has occurred. Howells *et al.* (2009) have shown that electron and X-ray diffraction and imaging data with resolutions ranging from 2 to 600 Å exhibit an empirical correlation between the sample lifetime and the resolution of a diffraction feature given by

$$\text{lifetime (MGy)} = 10 \times \text{resolution (Å)}. \qquad (1)$$

Assuming that the half dose scales with resolution in a similar way to the lifetime as defined by Howells and coworkers, our half dose of 64 MGy at a ribosome crystal diffraction resolution of 3 Å is then consistent (within the factor-of-two uncertainty mentioned above) with the reported half doses of 17 MGy at a resolution of 1.6 Å for tetragonal lysozyme crystals (Teng & Moffat, 2002), 21 MGy at 1.2 Å for myrosinase crystals (Burmeister, 2000) and 43 MGy at ~2.3 Å for ferritin crystals (Owen *et al.*, 2006). Howells and coworkers also reported resolution-dependent maximum tolerable doses for a ribosome crystal at 100 K having a much larger unit cell (a = b = 685 Å, c = 2690 Å), much lower initial diffraction resolution (17 Å) and a correspondingly much larger initial maximum dose (143 MGy). When the fit to the resolution-dependent maximum dose shown in Fig. 3 of Howells and coworkers is extrapolated to resolutions of 3–6 Å, lifetimes of 38–65 MGy are obtained, which is also consistent with the present result.

We thus conclude that the T = 100 K radiation sensitivity of the 70S ribosome crystal we examined is comparable, after resolution correction, to the 100 K sensitivity of other macromolecular crystals, including those of small model proteins, consistent with the current understanding of low-temperature global radiation damage both in macromolecular X-ray crystallography and in the broader fields of diffraction and cryomicroscopy utilizing ionizing radiation.

The present results highlight the implication of Howells and coworkers that there is no absolute maximum tolerable dose even at T = 100 K for protein crystallography experiments; instead, the maximum tolerable dose depends upon the available or desired resolution. Differences between earlier measurements of the T = 100 K half dose (a measure of the maximum tolerable dose) of ~20 MGy, a value often referred to as the 'Henderson limit', and a more recent value of 43 MGy are owing at least in part to differences in resolution

of the data sets used (1.2–1.6 *versus* 2.3 Å). Furthermore, the integrated intensity within a resolution shell decays more slowly with dose as the average resolution of the shell decreases, *i.e.* as the resolution in Å increases (Teng & Moffat, 2000; Sliz *et al.*, 2003). Consequently, if crystal diffraction is truncated to remove high-resolution peaks, the apparent half dose or maximum tolerable dose will be larger than if the full initial resolution of the diffraction of the crystal is included.

4.4. Radiation sensitivity at 180 K

The 70S ribosome crystal examined at T = 180 K was approximately eight times more sensitive than that at 100 K, as measured by both the half dose and the B-factor sensitivity (see Fig. 1). This factor of eight is four times larger than the factor of ∼2 measured for thaumatin (see Fig. 3). Since the ribosome crystals at 100 and 180 K diffracted to very nearly the same resolution, the resolution dependence of the half dose (discussed in §4.3 above) cannot explain the excess 180 K sensitivity.

One explanation for this excess sensitivity is that ribosome crystals have much larger solvent spaces (∼150 *versus* ∼30 Å) than thaumatin crystals. This may result in larger solvent, free-radical and protein mobility at T = 180 K than in thaumatin and thus in greater damage to ribosome crystals at 180 K relative to 100 K (where solvent, atomic and molecular radical and protein mobility are negligible.) Aqueous solvent confined to approximately nanometre-sized pores shows decreased mobility compared with the bulk. Both the melting point and the NMR relaxation time of water confined to porous glass show a strong dependency on pore size, with the former decreasing to ∼220 K as the pore diameter shrinks to ∼23 Å (Rault *et al.*, 2003). An onset of solvent mobility is observed in butyrylcholinesterase (42 Å channels) at 175 K, but a similar onset in tetragonal lysozyme (10–12 Å channels) does not appear until 190 K (Weik *et al.*, 2004). Devitrification (crystal formation within the solvent just above the glass-transition temperature) occurs at 155 K in the 65 Å pores of the trigonal form of acetylcholinesterase, but not in the 10 Å pores of the orthorhombic crystal form (Weik *et al.*, 2001). Consequently, a larger T = 180 K mobility of solvent and thus of free radicals and protein conformation in the ∼150 Å spaces in ribosome crystals than in the ∼30 Å channels of thaumatin crystals may account in part for the excess radiation sensitivity of the former at this temperature.

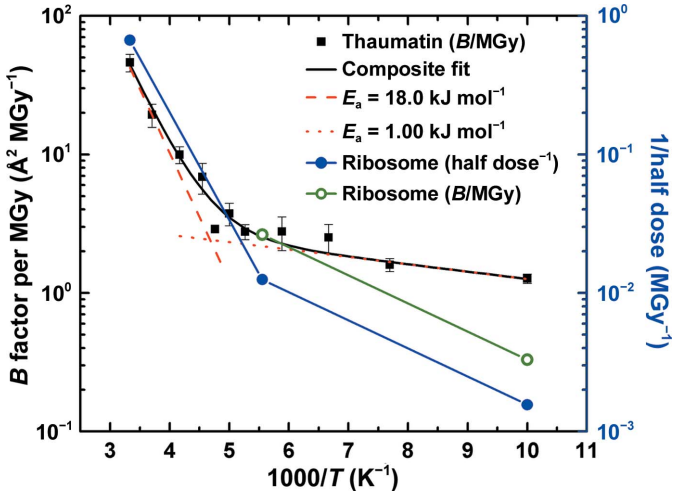

Figure 3
Half dose (solid blue circles, right scale) and B-factor sensitivity (open green circles, left scale) data for 70S ribosome crystals from the present work compared with B-factor sensitivity data for thaumatin crystals from Warkentin & Thorne (2010) (solid black squares, left scale). Between 180 and 300 K, the temperature dependence of the ribosome half dose roughly agrees with that of the thaumatin B-factor sensitivities. At lower temperatures, the ribosome data appear to be more strongly temperature dependent. This may result because solvent, free-radical and protein conformational mobility may persist to lower temperatures in ribosome crystals owing to the much larger solvent channels, moving the 'kink' separating the high-temperature and low-temperature regimes evident in the thaumatin data to lower temperatures.

4.5. Radiation sensitivity at 300 K

At room temperature, the 70S ribosome crystal had a half dose of 0.15 MGy. This is comparable to the reported half-dose values for thaumatin (0.24–0.42 MGy) and insulin (0.13–0.22 MGy) for data collected to 1.6 Å resolution (Rajendran *et al.*, 2011) and for native lysozyme crystals (typically 0.15–0.25 MGy) for data collected to 2 Å resolution (Barker *et al.*, 2009). The diffraction resolution of the ribosome crystal at 300 K was ∼5 Å. A lifetime–resolution relation similar to (1) has not been derived from room-temperature diffraction and imaging data. However, assuming the scaling of (1), a ribosome crystal initially diffracting to 1.6 Å resolution would have a half dose of ∼0.050 MGy, a few to several times smaller than that of model proteins. The ratio of room temperature to 100 K half doses is ∼430, or roughly 1000 after correcting for the lower average room-temperature resolution. This is roughly ten times larger than for model proteins (for which only independently published half-dose values at room temperature and 100 K are available) and can be compared with B-factor sensitivity ratios of 48 for lysozyme, 35 for thaumatin and 27 for apoferritin (Kmetko *et al.*, 2011).

The radiation sensitivities in Fig. 3 between 300 and 180 K can be fitted with an Arrhenius law (red dashed line for thaumatin and the left segment of the solid blue line for the ribosome). The slopes of these fits and thus the activation energies for thaumatin and ribosome crystals are comparable. This suggests that, within this temperature range of significant solvent and conformational mobility, a similar set of processes may be responsible for global radiation damage in both crystals.

4.6. Origin of the large radiation sensitivity of the 70S ribosome at 300 K

At T = 100 K, the radiation sensitivity of 70S ribosome crystals is comparable to that of crystals of model proteins such as lysozyme and thaumatin. However, at 300 K ribosome crystals are between three and ten times more sensitive, when account is taken of the differences in resolution. What could account for this excess sensitivity?

All proteins are made of the same amino acids and all RNAs are made of the same nucleotides. Even accounting for differences in the frequency of, for example, more radiation-sensitive residues such as cysteine and in the solvent exposedness of radiation-sensitive residues (which generally increases the probability per unit dose that they will be damaged at temperatures above ∼150 K; Filali-Mouhim *et al.*, 1997; Audette *et al.*, 2000; Juers & Weik, 2011; Warkentin, Badeau, Hopkins & Thorne, 2012), the underlying radiation chemistry and the rates of bond breaking and other chemical damage per unit dose, averaged over all atoms in the unit cell, should be similar for crystals of nearly all proteins and protein–RNA complexes. Possible exceptions include crystals with extremely high solvent contents (>90%), where protein damage owing to a preponderance of radicals being generated in the solvent may be expected to increase chemical damage per unit dose.

Large differences in room-temperature radiation sensitivity are more likely to be associated with conformational and other structural relaxation processes that occur downstream of radical reactions and chemical damage. These can involve much larger motions of much larger numbers of atoms than the bond breaking that precipitates them, and so should have a much larger effect on the overall decay of diffraction-spot intensities. Several factors may contribute to determining the extent of radiation-induced structural relaxations. Larger and/or more abundant solvent channels, cavities and packing imperfections may facilitate large motions of damaged side chains and local 'unfolding'. Conformational flexibility must also be important; radiation damage may, for example, shift the relative populations of alternative conformers. Weak crystal contacts/weak constraints on the position and orientation of a molecule in the crystal lattice may facilitate molecule-scale displacements and rotations.

As noted above, 70S ribosome crystals have very large solvent cavities. A smaller fraction of residues are involved in crystal contacts than in smaller proteins. However, in such a large and complex structure it is difficult to identify and especially to properly weight all of the structural elements that may contribute to radiation sensitivity. This is especially true because almost nothing is known about the structural relaxations that accompany radiation damage, aside from minor relaxations involving only a few atoms evident as 'site-specific damage'. Unless a large fraction of unit cells show the same structural relaxation, the relaxation cannot be identified in electron-density maps, even though it may cause a substantial loss of map resolution.

If the large 300 K sensitivity of 70S ribosome crystals is in fact largely owing to structural relaxations downstream of chemical damage, these crystals may be excellent candidates for damage reduction *via* ultrafast data collection. Near room temperature, free-radical diffusion and reaction is largely complete on microsecond timescales (Dertinger & Jung, 1970). However, structural relaxation processes occur on a range of timescales extending toward 1 s (Warkentin *et al.*, 2011). Recent experiments using ultra-intense synchrotron beams, fast framing detectors and crystals with modest room-temperature sensitivities have shown that manifested damage can be reduced by a factor of ∼2 by collecting data in ∼0.1–1 s (Owen *et al.*, 2012; Warkentin, Badeau, Hopkins, Mulichak *et al.*, 2012; Warkentin *et al.*, 2013). A larger fraction of the large room-temperature sensitivity of the ribsome is likely to be associated with (slow) structural rather than (fast) chemical relaxations, so fast data collection should yield even larger reductions in manifested damage.

5. Conclusions

We have investigated the dose, time and temperature dependence of radiation damage in 70S ribosome crystals. Their sensitivity to global X-ray damage is consistent with current understanding of global radiation damage at both 100 K and room temperature. Ribosome crystals are, after resolution corrections, comparably sensitive to small model proteins at T = 100 K, and roughly an order of magnitude more sensitive than small model proteins at room temperature. The data suggest that the processes and structural changes that determine global X-ray sensitivity have a modest dependence on macromolecular structure and size at room temperature, and that larger solvent spaces may allow appreciable solvent mobility and associated larger damage rates to persist to lower temperatures. A remarkable structural transformation in the MPD-stabilized ribosome crystals is brought on by cooling to temperatures below ∼200 K. This transformation increases the diffraction resolution from ∼5–10 to ∼3 Å.

The authors wish to acknowledge T. A. Steitz for his generous support and D. Bulkley for providing the ribosome crystals. This work was supported by the National Science Foundation (NSF) under award MCB 1330685 (Cornell) and by the National Institutes of Health (NIH) under awards R01GM065981 (Cornell) and P01 GM022778 (Yale). Use of the National Synchrotron Light Source, Brookhaven National Laboratory was supported by the US Department of Energy, Office of Science, Office of Basic Energy Sciences under Contract No. DE-AC02-98CH10886. RET acknowledges a significant financial interest in MiTeGen LLC, the vendor of some of the tools used in these experiments.

References

Audette, M., Chen, X., Houée-Levin, C., Potier, M. & Le Maire, M. (2000). *Int. J. Radiat. Biol.* **76**, 673–681.
Barker, A. I., Southworth-Davies, R. J., Paithankar, K. S., Carmichael, I. & Garman, E. F. (2009). *J. Synchrotron Rad.* **16**, 205–216.
Blake, C. & Phillips, D. C. (1962). *Proceedings of the Symposium on the Biological Effects of Ionising Radiation at the Molecular Level*, pp. 183–191. Vienna: International Atomic Energy Agency.
Burmeister, W. P. (2000). *Acta Cryst.* D**56**, 328–341.
Chapman, H. N. *et al.* (2011). *Nature (London)*, **470**, 73–77.
Dertinger, H. & Jung, H. (1970). *Molecular Radiation Biology*. Berlin: Springer-Verlag.
Dobrianov, I., Kriminski, S., Caylor, C. L., Lemay, S. G., Kimmer, C., Kisselev, A., Finkelstein, K. D. & Thorne, R. E. (2001). *Acta Cryst.* D**57**, 61–68.
Edayathumangalam, R. S. & Luger, K. (2005). *Acta Cryst.* D**61**, 891–898.

Esnouf, R. M., Ren, J., Garman, E. F., Somers, D. O'N., Ross, C. K., Jones, E. Y., Stammers, D. K. & Stuart, D. I. (1998). *Acta Cryst.* D**54**, 938–953.
Filali-Mouhim, A., Audette, M., St-Louis, M., Thauvette, L., Denoroy, L., Penin, F., Chen, X., Rouleau, N., Le Caer, J.-P., Rossier, J., Potier, M. & Le Maire, M. (1997). *Int. J. Radiat. Biol.* **72**, 63–70.
Fraser, J. S., Clarkson, M. W., Degnan, S. C., Erion, R., Kern, D. & Alber, T. (2009). *Nature (London)*, **462**, 669–673.
Fraser, J. S., van den Bedem, H., Samelson, A. J., Lang, P. T., Holton, J. M., Echols, N. & Alber, T. (2011). *Proc. Natl Acad. Sci. USA*, **108**, 16247–16252.
Henderson, R. (1990). *Proc. R. Soc. Lond. B. Biol. Sci.* **241**, 6–8.
Howells, M. R., Beetz, T., Chapman, H. N., Cui, C., Holton, J. M., Jacobsen, C. J., Kirz, J., Lima, E., Marchesini, S., Miao, H., Sayre, D., Shapiro, D. A., Spence, J. C. & Starodub, D. (2009). *J. Electron. Spectros. Relat. Phenomena*, **170**, 4–12.
Juers, D. H. & Weik, M. (2011). *J. Synchrotron Rad.* **18**, 329–337.
Kabsch, W. (2010). *Acta Cryst.* D**66**, 125–132.
Kiefersauer, R., Than, M. E., Dobbek, H., Gremer, L., Melero, M., Strobl, S., Dias, J. M., Soulimane, T. & Huber, R. (2000). *J. Appl. Cryst.* **33**, 1223–1230.
Kmetko, J., Husseini, N. S., Naides, M., Kalinin, Y. & Thorne, R. E. (2006). *Acta Cryst.* D**62**, 1030–1038.
Kmetko, J., Warkentin, M., Englich, U. & Thorne, R. E. (2011). *Acta Cryst.* D**67**, 881–893.
Meents, A., Wagner, A., Schneider, R., Pradervand, C., Pohl, E. & Schulze-Briese, C. (2007). *Acta Cryst.* D**63**, 302–309.
Otwinowski, Z. & Minor, W. (1997). *Methods Enzymol.* **276**, 307–326.
Owen, R. L., Axford, D., Nettleship, J. E., Owens, R. J., Robinson, J. I., Morgan, A. W., Doré, A. S., Lebon, G., Tate, C. G., Fry, E. E., Ren, J., Stuart, D. I. & Evans, G. (2012). *Acta Cryst.* D**68**, 810–818.
Owen, R. L., Rudiño-Piñera, E. & Garman, E. F. (2006). *Proc. Natl Acad. Sci. USA*, **103**, 4912–4917.
Paithankar, K. S. & Garman, E. F. (2010). *Acta Cryst.* D**66**, 381–388.
Rajendran, C., Dworkowski, F. S. N., Wang, M. & Schulze-Briese, C. (2011). *J. Synchrotron Rad.* **18**, 318–328.
Rault, J., Neffati, R. & Judeinstein, P. (2003). *Eur. Phys. J. B*, **36**, 627–637.
Schulze-Briese, C., Wagner, A., Tomizaki, T. & Oetiker, M. (2005). *J. Synchrotron Rad.* **12**, 261–267.
Selmer, M., Dunham, C. M., Murphy, F. V., Weixlbaumer, A., Petry, S., Kelley, A. C., Weir, J. R. & Ramakrishnan, V. (2006). *Science*, **313**, 1935–1942.
Sliz, P., Harrison, S. C. & Rosenbaum, G. (2003). *Structure*, **11**, 13–19.
Southworth-Davies, R. J., Medina, M. A., Carmichael, I. & Garman, E. F. (2007). *Structure*, **15**, 1531–1541.
Teng, T. & Moffat, K. (2000). *J. Synchrotron Rad.* **7**, 313–317.
Teng, T.-Y. & Moffat, K. (2002). *J. Synchrotron Rad.* **9**, 198–201.
Warkentin, M., Badeau, R., Hopkins, J. B., Mulichak, A. M., Keefe, L. J. & Thorne, R. E. (2012). *Acta Cryst.* D**68**, 124–133.
Warkentin, M., Badeau, R., Hopkins, J. & Thorne, R. E. (2011). *Acta Cryst.* D**67**, 792–803.
Warkentin, M., Badeau, R., Hopkins, J. B. & Thorne, R. E. (2012). *Acta Cryst.* D**68**, 1108–1117.
Warkentin, M., Hopkins, J. B., Badeau, R., Mulichak, A. M., Keefe, L. J. & Thorne, R. E. (2013). *J. Synchrotron Rad.* **20**, 7–13.
Warkentin, M. & Thorne, R. E. (2010). *Acta Cryst.* D**66**, 1092–1100.
Weik, M., Kryger, G., Schreurs, A. M. M., Bouma, B., Silman, I., Sussman, J. L., Gros, P. & Kroon, J. (2001). *Acta Cryst.* D**57**, 566–573.
Weik, M., Vernede, X., Royant, A. & Bourgeois, D. (2004). *Biophys. J.* **86**, 3176–3185.